

# An MCNP™ Based Method to Determine the Matrix Attenuation Correction Factors for a Gamma Box Counter

H. Zhu, S. Croft, R. Venkataraman and S. Philips  
Canberra Industries, Inc., 800 Research Parkway, Meriden, Connecticut, 06450, U.S.A.

## Abstract

A general purpose Gamma Box Counter is a large scale, high-resolution segmented gamma-ray nondestructive assay system for the assay of nuclear waste containers covering a wide range of composition, mass, and geometry. In order to accurately quantify the activity of the radionuclides in a waste container, a correction for the gamma-ray self-attenuation in the waste matrix must be estimated and applied. One of the methods of determining the self-attenuation involves measuring the transmission through the matrix using gamma-rays from an external source. Assuming each segment of the matrix is uniform, the matrix attenuation correction factor can be expressed as a function of the transmission governed by a geometry dependent parameter  $\kappa$ . The parameter  $\kappa$  is a scale parameter applied to the characteristic thickness (or diameter) in the model function, and can vary for different waste container shapes. To determine the parameter  $\kappa$  for the different waste containers in the application of interest, the transmission ratio and attenuation correction factor must be known for each container at a variety of energies. This information can be acquired experimentally but can also be obtained using a transport code to simulate the behavior. In this application simulations also serve to enhance understanding of the problem, provide confidence in the solution by experimental benchmarking, and provide an alternative in the case of difficult-to-measure scenarios.

## Introduction

This Segmented Gamma Box Counter (SGBC) system is intended to assay large waste containers such as the Standard Waste Box<sup>[1]</sup> (SWB), Standard Large Box-2<sup>[1]</sup> (SLB-2), and Ten Drum Over-Pack<sup>[1]</sup> (TDOP) for direct quantification of <sup>241</sup>Am, <sup>238</sup>Pu, <sup>239</sup>Pu, <sup>240</sup>Pu, <sup>241</sup>Pu, <sup>242</sup>Pu, <sup>233</sup>U, <sup>234</sup>U, <sup>235</sup>U, <sup>238</sup>U, <sup>90</sup>Sr, <sup>137</sup>Cs, <sup>237</sup>Np, and other radionuclides using transmission calibration or efficiency multi-curve<sup>[2]</sup> to compensate for variations in matrix density. The operation of the system is illustrated in Figure 1. It has a moving item trolley which runs on rails past two counting stations, one station for passive emission counting, and the other for transmission counting. The sample trolley moves between two detector towers on

which are mounted a total of four High-Purity Germanium (HPGe) detectors – two detectors mounted one above the other on the left-hand tower, and two mounted on the right-hand tower. Located roughly two meters further down the rails, past the passive station, is the transmission station. Here, the sample trolley moves between two additional towers. On the left-hand tower are mounted two large (5 inch diameter by 4 inch deep), temperature-stabilized NaI(Tl)(Tl) detectors. On the right-hand tower are mounted two very large lead pigs each housing a <sup>60</sup>Co transmission source of nominally 250 mCi. Each pig has an automated assembly with two tungsten pieces which can be independently actuated to move them in/out of the shine path of the source. One tungsten piece, the shutter, is 7” long and 2” in diameter. The other tungsten piece, the attenuator, is 1.2” long and 2” in diameter. The long sintered tungsten piece serves as the beam shutter. The short piece control the intensity between a low beam for light matrix and a high beam for dense matrix. The control is needed to keep count rate below the limit of the NaI(Tl) detector system. During waste assay, the transmission scan will take place first at several container-dependent discreet positions of the trolley. At each position two NaI(Tl) transmission acquisitions will take place simultaneously – one for the upper NaI(Tl), and one for the lower NaI(Tl). The passive emission scan

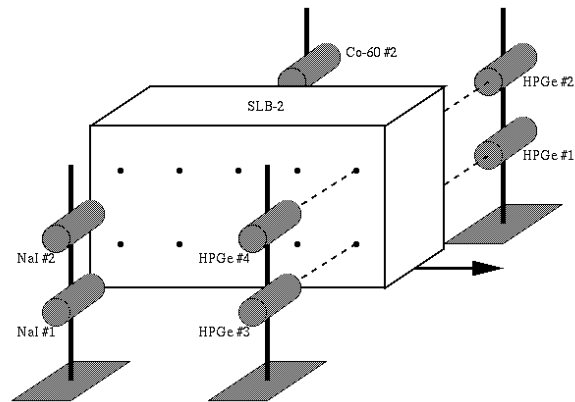


**Figure 1.** Illustration of the operations of the SGBC Gamma Box Counter.

will take place simultaneously – one for the upper NaI(Tl), and one for the lower NaI(Tl). The passive emission scan

will take place with the same number of discrete positions as with the transmission measurements. Both scans take place so that the transmission beams and the centerlines of the HPGe detectors hit the sample container at the same places. The system is to be analyzed like a Segmented Gamma Scanner (SGS)<sup>[3][4]</sup> – each segment's peak count rate data will be corrected for transmission to a “zero” density count rate, and then analyzed.

Suppose the waste item being assayed is a container with homogeneous matrix of uniform activity distribution. Due to matrix attenuation in the container, the apparent assay result (activity or mass) at each gamma ray line of the radionuclide waste will be biased low when the appropriate empty container calibration is assumed. The apparent mass of the radionuclides is multiplied by a Correction Factor ( $CF_{Matrix}$ ) in order to get the assay value compensated for matrix attenuation. In the ideal world of theoretical simulations  $CF_{Matrix}$  may be computed from the ratio of

$$CF_{Matrix} = \frac{\varepsilon_{Empty}}{\varepsilon_{Matrix}} \quad (1)$$

where  $\varepsilon_{Empty}$  and  $\varepsilon_{Matrix}$  is the HPGe detector efficiency for the empty container and the container with waste matrix, respectively. To a good approximation the computation of this ratio is independent of the properties of the actual HPGe detector being primarily a function of the transport of radiation inside the matrix itself. The container wall is a second order effect for slant angles, for the detection of interest here the dead layer is negligible and filter are optional. In the SGBC geometry the detector response as a function of the angular pattern of incoming rays is also very much secondary. Therefore, the measurement efficiency of the empty container and the container with matrix can be calculated mathematically if the HPGe detectors are efficiency characterized.

Empirically, the matrix self-attenuation correction factor can also be parameterized in terms of the measured transmission ratio between the empty container and the container with matrix. The two semi-empirical forms of practical interest are the effective slab and the effective sphere which represent closed form expression for the shapes of the waste containers.

In the case of the far field approximation where the maximum dimensions of both the sample and the detector are negligible compared with their separation, the parameterization for the case of effective slab is given by Parker<sup>[5]</sup>

$$CF_{Matrix} = \frac{\kappa \cdot x}{1 - e^{-\kappa \cdot x}} \quad (2)$$

where  $x$  is the optical thickness of the slab and  $\kappa$  is a sample container geometry-dependent parameter. For 208-liter sample drums, the  $\kappa$  factor can be thought of as the factors by which the diameter must be multiplied by in order to obtain the mean path length of the emerging photons out of the cylindrical surface of a uniform disk. For a cylinder,  $\kappa$  is about 0.8 for an SGS while for a true slab viewed in far field geometry one would expect a value of close to unity.

The parameterization for the case of effective sphere in the far field is parameterized by Croft<sup>[6]</sup>

$$CF_{Matrix} = \frac{(\kappa \cdot x)^3 / 3}{(\kappa \cdot x)^2 / 2 - 1 + (1 + \kappa \cdot x)e^{-\kappa \cdot x}} \quad (3)$$

where  $x$  is the diametrical optical thickness of the sphere and  $\kappa$  is the sample container geometrical parameter for this model. In this case  $\kappa$  becomes a multiplicative factor for the container dimensions relative to the effective length of a sphere to obtain the effective mean path length of the emerging photon, thus for a fictional spherical sample container in the far field, the value should be unity.

In both parameterizations, for a given material at a given energy, the value of  $x$  is directly proportional to the matrix density. But in the case of a narrow beam transmission measurement we may use the relations  $x = \ln(1/T)$  in the expressions (2) and (3), where  $T$  is the transmission ratio at the assay energies. In the case of the SGBC, the estimate of the transmission ratio  $T$  is not taken in narrow beam geometry because the use of a pair of NaI(Tl) detectors which accept events that have suffered small angle scattering in the container matrix. Furthermore, the transmission is not available at the assay energy but only at the energies of <sup>60</sup>Co. Because of these issues, if more sophisticated estimated are needed than can be obtained by using the simple exponential attenuation equation to be used to obtain the transmission ratio, one must resort to using Monte Carlo simulations. However, the effects are minor in practice

and are readily calibrated out. The transmission at other energies may also be readily estimated with the knowledge of the energy dependence of the mass attenuation coefficient (MAC) and the matrix composition.

### Evaluation of the $\kappa$ Values

From Equations (2) and (3), in order to determine  $\kappa$  values for various waste containers used in SGBC, the matrix self-attenuation correction factor ( $CF_{Matrix}$ ) and the transmission ratio ( $T$ ) must be known.

The matrix self-attenuation correction ( $CF_{Matrix}$ ) is calculated based on the HPGe detector efficiencies for various containers and matrices. Because the HPGe detectors are efficiency characterized, under the assumption of uniform container matrix, the HPGe detector efficiencies for various containers can be calculated using Canberra's In Situ Object Calibration Software (ISOCS<sup>[7]</sup>) tool. Since the SGBC is operated in SGS mode, four HPGe detectors in opposing pairs are modeled in ISOCS at various container-dependent discrete scanning positions. The efficiency calculations are performed at multiple gamma ray energies (100, 129, 186, 414, 1001, 1173 and 1332 keV) for the 208-liter drum (the closest approximation to the far field), SWB, SLB-2 and TDOP containers with various densities assuming uniform container matrix. The container matrix materials was taken to be cellulose at low to medium densities (up to 0.60 g/cm<sup>3</sup>) and high density polyethylene (HDPE) or silica (SiO<sub>2</sub>) at medium to high densities (up to 1.5 g/cm<sup>3</sup>). The efficiency sum of the four HPGe detectors at all scanning positions were used to calculate the matrix attenuation correction factor. The ISOCS calculations of the HPGe detector efficiency were benchmarked by measurements during the experimental calibration<sup>[8]</sup>, a very good agreement (typically within 5% across all energies) in the absolute detector efficiency was achieved. Since the matrix self-attenuation correction factor is the ratio of the efficiency, the uncertainty in the ISOCS calculated efficiency is largely canceled out, hence the error analysis for the correction factor is not discussed in this paper. The correction factors computed by ISOCS at various container matrices and gamma ray energies are presented in Table 1.

**Table 1.** Correction factors for various container matrices and gamma ray energies computed by ISOCS.

Container	Density (g/cm <sup>3</sup> )	Energy (keV)							
		1332	1173	1001	662	414	186	129	100
208-liter drum	0.0012	1	1	1	1	1	1	1	1
	0.05	1.0627	1.0665	1.0698	1.0874	1.1071	1.1434	1.1641	1.1769
	0.47	1.7624	1.8145	1.9000	2.1261	2.4172	2.9904	3.2982	3.5020
	0.72	2.2390	2.3314	2.4611	2.8427	3.3244	4.2779	4.7475	5.1032
	1.52	3.8321	4.0505	4.3578	5.1986	6.2312	8.3378	9.5190	6.2795
	2	4.7594	5.0440	-	-	-	-	-	-
SWB	0.0012	1	1	1	1	1	1	1	1
	0.13	1.4555	1.4889	1.5330	1.6629	1.8281	2.1383	2.2885	2.4020
	0.3	2.1463	2.2355	2.3506	2.6825	3.0952	3.8921	4.2806	4.5524
	0.6	3.4734	3.6682	3.9016	4.6082	5.4545	7.0812	7.8600	8.4155
	0.9	4.6387	4.8909	5.2308	6.2288	7.4522	10.0185	11.7126	13.6182
SLB-2	0.0012	1	1	1	1	1	1	1	1
	0.13	1.6261	1.6773	1.7415	1.9355	2.1779	2.6391	2.8808	3.0417
	0.3	2.6755	2.8014	2.9774	3.4761	4.1040	5.2781	5.8389	6.2527
	0.6	4.6954	4.9686	5.3353	6.3594	7.6619	10.0225	11.1253	11.9672
	0.9	6.4455	6.8103	7.3254	8.7898	10.6500	14.3871	16.7954	19.5973
TDOP	0.0012	1	1	1	1	1	1	1	1
	0.13	1.6017	1.6481	1.7106	1.8815	2.1146	2.5714	2.8017	2.9844
	0.3	2.5642	2.6970	2.8622	3.3333	3.9618	5.1818	5.7829	6.2426
	0.6	4.5081	4.7923	5.1560	6.1714	7.4775	9.9708	11.1684	12.1264
	0.9	6.5304	6.9531	7.5026	9.0756	10.9934	14.7414	16.5816	18.0342

The transmission ratio ( $T$ ) for gamma rays through various container matrices and detected by a 5" x 4" NaI(Tl) detector can be either experimentally measured, or it can be modeled through Monte Carlo simulations. When the gamma ray energy is very low and the container matrix is very dense, the experimental method may become impractical in terms of measurement time and source strength. In such cases, the transmission ratio can be modeled by simulations and the simulation tools can be benchmarked at measurable gamma ray energies. To this end, a MCNP<sup>[9]</sup> model has been developed to calculate the transmission ratio through various container matrix.

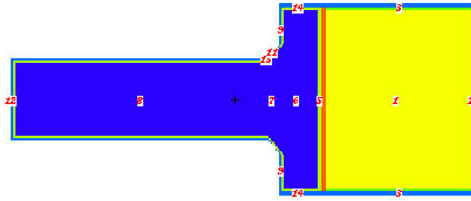


**Figure 2.** MCNP model of a 5'' x 4'' NaI(Tl).

The MCNP model for a 5'' x 4'' NaI(Tl) detector is shown in Figure 2. The model includes the active material of the 99.8% NaI(Tl) doped with 0.2% of TlI and other components such as MgO oxide for specular reflection, Plexiglas/Acrylic optical interface, glass (SiO<sub>2</sub>) photocathode, aluminum, stainless steel shells, etc. Gaussian broadening with a realistic NaI(Tl) detector energy resolution (the Full Width at Half Maximum in [MeV] =  $-0.0114 + 0.0673 \cdot \sqrt{E}$ ) is used to generate the NaI(Tl) photo-peaks. The transmission ratio calculation model has assumed that the axis of the transmission source and the NaI(Tl) detector aligned with the center of the container except for the case of the TDOP container where transmission ratio calculation takes place at three scanning positions due to the difference in average photon path length at different scanning positions, i.e. the curvature of the TDOP matters while the other containers are blocks. Calculations are performed at multiple gamma ray energies, i.e. 100, 129, 186, 414, 1001, 1173 and 1332 keV. The calculation can be CPU intensive especially for low energy gamma rays. In order to reduce the computation time, a cutoff energy window with region of interest (ROI) equals [peak energy - 2\*FWHM, peak energy + 2\*FWHM] is applied. For instance, for <sup>60</sup>Co gamma ray energies, the ROI in the simulation is set at twice the FWHM of the 1173 keV line to the left of the peak and twice the FWHM of the 1332 peak to the right of the peak, so that transmission ratio can be calculated either for each peak or for the sum of the two peaks. The statistical uncertainty of the efficiencies reported by MCNP for each peak is typically sufficiently small (much less than 2% for all densities) and therefore no sophisticated error analysis is required. The MCNP calculated transmission ratio for various containers matrices and gamma ray energies are shown in Table 2.

**Table 2.** Transmission ratios for various container matrices and gamma ray energies computed by MCNP model.

Container	Density (g/cm <sup>3</sup> )	Energy (keV)							
		1332	1173	1001	662	414	186	129	100
208-liter drum	0.0012	1	1	1	1	1	1	1	1
	0.05	8.53E-01	8.42E-01	8.29E-01	7.96E-01	7.56E-01	6.88E-01	6.58E-01	6.36E-01
	0.47	2.09E-01	1.90E-01	1.64E-01	1.12E-01	6.85E-02	2.79E-02	1.82E-02	1.33E-02
	0.72	9.13E-02	7.86E-02	6.27E-02	3.48E-02	1.65E-02	4.15E-03	2.15E-03	1.32E-03
	1.52	8.36E-03	6.28E-03	4.23E-03	1.21E-03	2.87E-04	7.58E-06	-	6.73E-05
2	1.82E-03	1.28E-03	-	-	-	-	-	-	-
SWB	0.0012	1	1	1	1	1	1	1	1
	0.13	3.77E-01	3.55E-01	3.23E-01	2.54E-01	1.88E-01	1.07E-01	8.19E-02	6.76E-02
	0.3	1.04E-01	9.06E-02	7.30E-02	4.19E-02	2.06E-02	5.58E-03	3.04E-03	1.94E-03
	0.6	1.08E-02	8.14E-03	5.29E-03	1.76E-03	4.33E-04	2.78E-05	-	-
	0.9	1.12E-03	7.58E-04	3.98E-04	7.05E-05	7.51E-06	-	-	-
SLB-2	0.0012	1	1	1	1	1	1	1	1
	0.13	2.93E-01	2.72E-01	2.41E-01	1.78E-01	1.21E-01	5.96E-02	4.29E-02	3.33E-02
	0.3	5.84E-02	4.86E-02	3.71E-02	1.83E-02	7.55E-03	1.47E-03	6.70E-04	3.65E-04
	0.6	3.36E-03	2.37E-03	1.39E-03	3.50E-04	5.32E-05	-	-	-
	0.9	1.92E-04	1.19E-04	5.12E-05	-	-	-	-	-
TDOP	0.0012	1	1	1	1	1	1	1	1
	0.13	2.90E-01	2.69E-01	2.39E-01	1.76E-01	1.20E-01	5.85E-02	4.19E-02	3.24E-02
	0.3	5.73E-02	4.74E-02	3.62E-02	1.78E-02	7.29E-03	1.40E-03	6.36E-04	3.49E-04
	0.6	3.21E-03	2.28E-03	1.32E-03	3.31E-04	4.98E-05	-	-	-
	0.9	1.79E-04	1.12E-04	4.85E-05	-	-	-	-	-

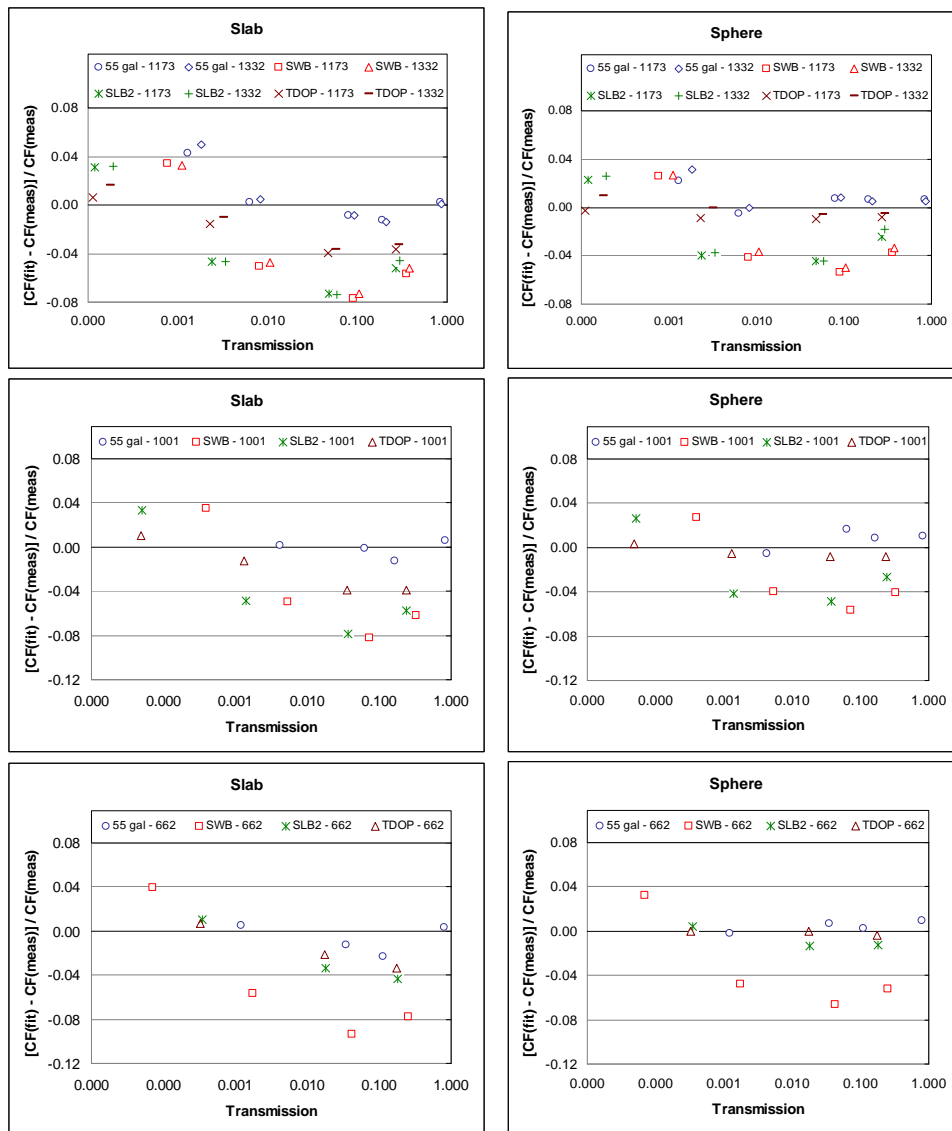
Two fitting models, modified from the far-field form of the attenuation correction for a slab and sphere, are used to derive  $\kappa$  values for each waste container type through  $\chi^2$  minimization using Solver tool in MS Excel assuming equal weight at each energy and density. For each container type, the extracted  $\kappa$  values at different gamma ray energies

and the combined  $\kappa$  values are shown in Table 3. The combined  $\kappa$  values are the best fit values when data at all energies are treated as a grand ensemble.

**Table 3.**  $\kappa$  values for different containers in slab and sphere parameterizations.

Model	Container	Energy (keV)								Combined
		1332	1173	1001	662	414	186	129	100	
"Slab"	208-liter drums	0.7853	0.7865	0.7878	0.7737	0.7665	0.7206	0.7718	0.7696	0.7680
	SWB	0.6990	0.6993	0.6882	0.6763	0.6582	0.6869	0.7341	0.7277	0.6958
	SLB-2	0.7759	0.7767	0.7660	0.8063	0.7882	0.8101	0.8034	0.7953	0.7922
	TDOP	0.7645	0.7713	0.7630	0.7737	0.7616	0.7877	0.7873	0.7870	0.7755
"Sphere"	208-liter drums	1.1175	1.1223	1.1279	1.1173	1.1153	1.0598	1.1124	1.1131	1.1094
	SWB	1.0059	1.0089	0.9961	0.9860	0.9658	1.0064	1.0542	1.0484	1.0097
	SLB-2	1.1323	1.1356	1.1229	1.1761	1.1573	1.1748	1.1703	1.1615	1.1567
	TDOP	1.1150	1.1275	1.1184	1.1271	1.1172	1.1411	1.1459	1.1491	1.1315

Based on the extracted  $\kappa$  value for each container, the correction factors are then calculated from each parameterization model and their relative deviations from the correction factor computed by the ISOCS is graphed in Figure 3.



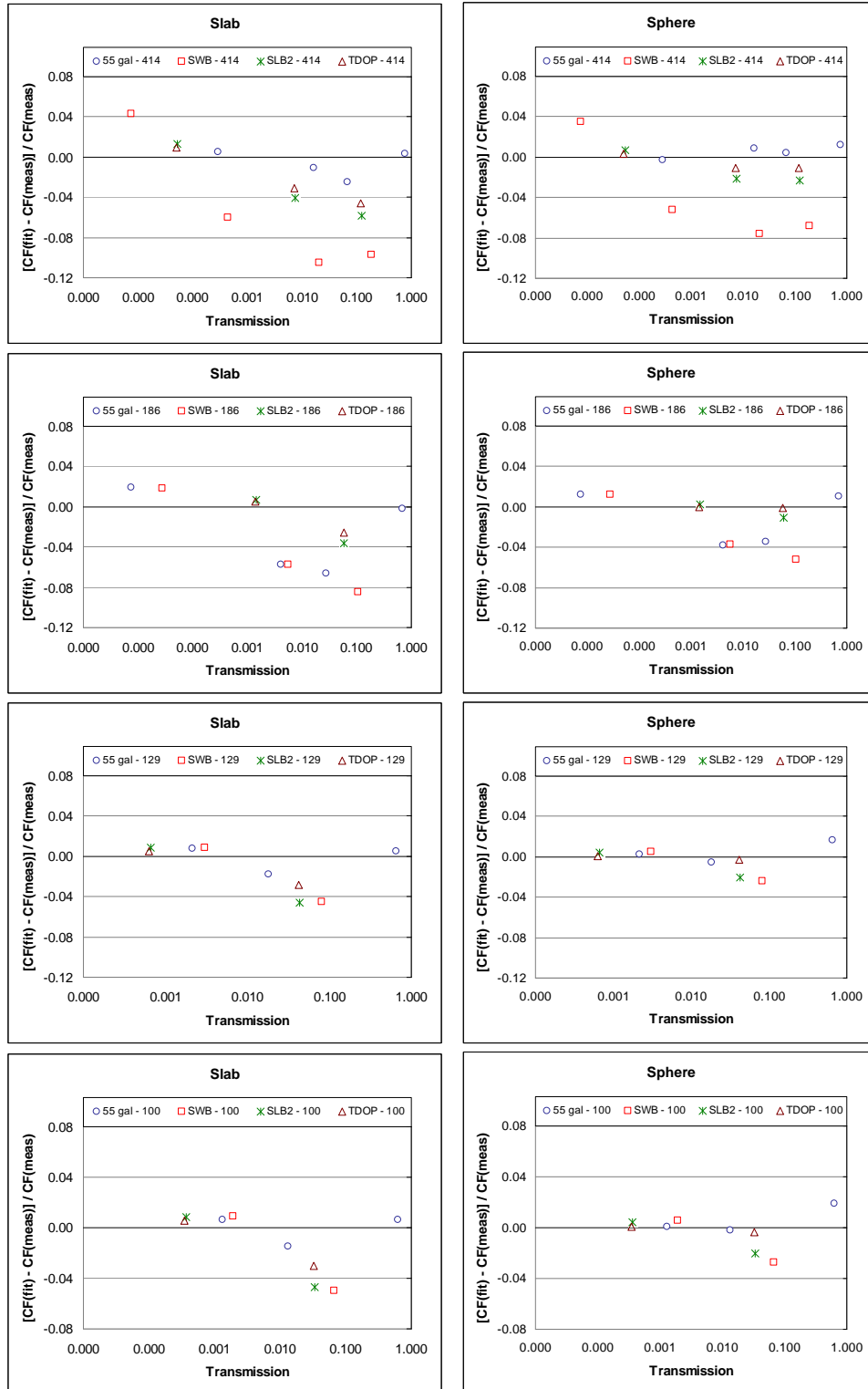


**Figure 3.** Deviation of the modeled to the ISOCS correction factors as function of the gamma ray energies and transmission ratio. The left (right) panel is for slab (sphere) model.

## Transmission Ratio Confirmatory Measurements

The model calculation for the transmission ratio is benchmarked by measurements in a pair of NaI(Tl) detectors each with its own 250 mCi  $^{60}\text{Co}$  transmission source. The measurements are only conducted with the  $^{60}\text{Co}$  transmission sources at 1173 and 1332 keV. The measurements are performed for 208-liter drum, SWB and SLB-2 container with various matrices. For low density matrix (including empty container), the 1.2" sintered tungsten attenuator is in the transmission shine path to avoid saturating the NaI(Tl) detectors, while for dense matrix, there is no attenuator in the beam path. Therefore, in order to calculate the transmission ratio relative to the empty container, the attenuation power or the MAC of the sintered tungsten must be known.

The mass attenuation coefficient of the sintered tungsten is determined by measuring the count rate in the NaI(Tl) detectors with the  $^{60}\text{Co}$  transmission sources for attenuator opened/closed modes. The net peak count rate (dead time loss corrected) of the 1173 and the 1332 keV are used to derive the apparent attenuator MAC. The experimentally determined MAC for the sintered tungsten is  $0.0537 \text{ cm}^2/\text{g}$ .

With known attenuator power, it is straight forward to measure the transmission ratio. Table 4 shows the measured transmission ratios and are compared to the MCNP calculated transmission ratios in one of the NaI(Tl) detectors for a 208-liter drum, SWB and SLB-2 containers. Similar results were obtained for the other NaI(Tl) detector. The only difference between the MCNP model and the benchmark measurement is that MCNP models assumed transmission beam punch through the center of the drum/container, while the benchmark measurement had two NaI(Tl) detector centered on the top and bottom half of the drum/container. Background count rate under the 1173 and 1332 peaks are negligible compared to the photo-peaks. The counting statistical error is approximately 5% for the most dense matrix with data acquisition time of several minutes for the empty drum/container and on approximately 10 minutes for the containers with dense matrix.

**Table 4.** Transmission ratio benchmark measurement and comparison to MCNP modeled results. The result is for the bottom NaI(Tl) detector SAP 953 (or the bottom detector). Volume fractions are shown for the SWB matrices.

Container	Matrix	Density (g/cm <sup>3</sup> )	1173 keV		1332 keV	
			Transmission ratio	Measurement MCNP	Transmission ratio	Measurement MCNP
208-liter drum	Empty	0.0129	1		1	
	Foam	0.045	9.27E-01	1.08	9.21E-01	1.06
	Homasote	0.473	1.90E-01	1.00	2.05E-01	0.98
	Particle Board	0.725	8.13E-02	1.03	9.36E-02	1.03
	Sand	1.540	5.71E-03	0.98	7.46E-03	0.95
SWB	Empty	0.0129	1		1	
	Cardboard	0.152	3.30E-01	1.02	3.51E-01	1.01
	40% Plywood + 60% Cardboard	0.270	1.18E-01	1.03	3.77E-01	1.01
	30% Polyethylene + 50% Plywood + 20% Cardboard	0.540	1.37E-02	1.05	1.80E-02	1.07
	81% Polyethylene + 19% Plywood	0.760	1.42E-03	0.96	2.01E-03	0.97
SLB-2	Empty	0.0129	1		1	
	Plywood	0.530	5.14E-03	1.06	7.26E-03	1.11

The matrix density had some uncertainty based on the dimensions of the matrix modules were used, the values listed in the Table 4 are our best estimates. Dependency on the matrix density could be quite dramatic particularly for the densest matrices. Nevertheless, the MCNP modeled transmission ratio and the confirmatory measurement results show rather impressive agreement. This validates the model we used to extract the  $\kappa$  values for all containers.

## Discussions

The  $\kappa$  values depend on the container geometry and the container to detector distance. For a fixed container geometry, its  $\kappa$  value will be fixed. Our study shows the combined (average)  $\kappa$  values do not seem to indicate a very strong dependence on the container types.

For the two parameterization models we used in this study, the overall bias  $(CF_{fit} - CF_{meas}) / CF_{meas}$  is -2.12% and 0.99% for the slab and the sphere model, respectively. The sphere model appears to have better fitting average all energies and transmission ratios.

Based on the results presented in this paper, similar to emission-efficiency multi-curve, a transmission ratio multi-curve, i.e. transmission ratio as function of energy and matrix density,  $T(E, \rho)$  can be built for a particular system under the assumption of uniform known matrix. A transmission multi-curve can be created based on MCNP simulations once the simulation is validated against benchmark measurements. A sample transmission multi-curve for the 208-liter drum, SWB, SLB-2 and TDOP containers are given in Figure 4.

This transmission ratio multi-curve can be readily used for matrix self-attenuation correction calculations when the matrix density and the gamma ray energy are known. For the application of the SGBC system, the transmission ratio ( $T$ ) is measured at  $^{60}\text{Co}$  energies, 1173 and 1332 keV, in order to obtain the transmission ratio at any other energies, extrapolations based on known MAC is required. If a transmission multi-curve is created based on simulation and benchmarked, then from the measured transmission ratio at  $^{60}\text{Co}$  energies and with known matrix densities, the transmission ratio can be readily interpolated to any other energies, from where the matrix correction factors ( $CF_{Matrix}$ ) can readily computed.

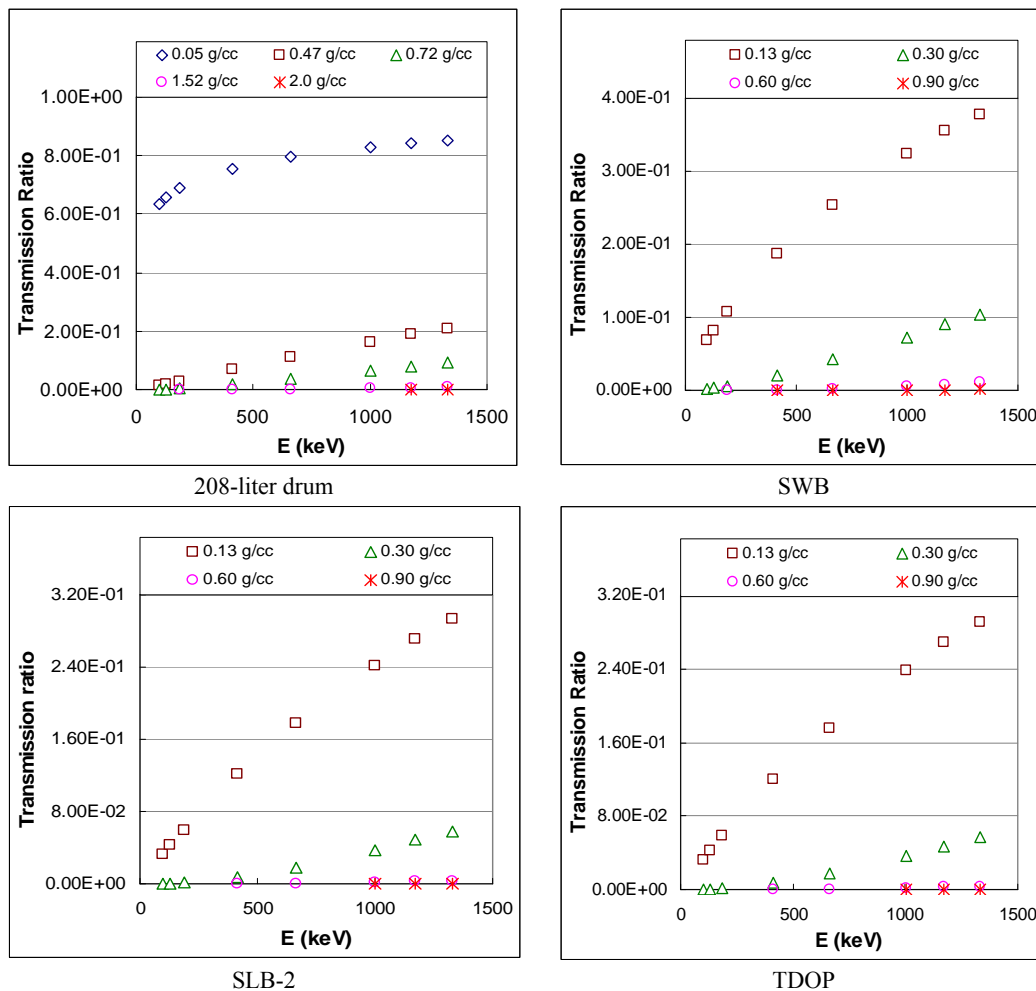


**Figure 4.** Transmission Multi-curve,  $T(E, \rho)$  for different container types.



## Acknowledgement

This work is supported by the Department of Energy under contract DE-AC09-04SR22389.

## References

- (1) "Specification for Fabrication of the Standard Waste Box, Standard Large Box 2 and Ten Drum Overpack", Washington TRU Solutions, LLC. Carlsbad, NM 88220.
- (2) M. Henry, et al, "Representing Full-Energy Peak Gamma-ray Efficiency Surfaces in Energy and Density when the Calibration Data is Correlated", WM'07 Conference, February 25-March 1, 2007, Tucson, AZ.
- (3) S. Croft, et al., "Quantifying SGS Matrix Correction Factor Uncertainties for Non-uniform Source Distributions", 45<sup>th</sup> INMM Conference.
- (4) ASTM Standard Test Method Designation C 1133, "Nondestructive Assay of Special Nuclear Material in Low-Density Scrap and Waste by Segmented Passive Gamma-Ray Scanning".
- (5) J. Parker, "A Correction for Gamma Ray Self-Attenuation in Regular Heterogeneous Materials", LA-UR-87-3954, Los Alamos National Laboratory, 1987.
- (6) S. Croft, *Nucl. Geophys.* 9(1995)425.
- (7) R. Venkataraman, F. Bronson, V. Atrashkevich, B. M. Young, and M. field, "Validation of in situ object counting system (ISOCS) mathematical efficiency calibration software," *Nucl. Inst. and Meth. in Phys. Res.*, A442 (1999) 450.
- (8) H. Zhu, "Savannah River Gamma Box Counter Calibration Report", Canberra Industries, Inc., April 2007.
- (9) X-5 Monte Carlo Team, "MCNP – A General Monte Carlo N-Particle Transport Code, Version 5," LANL Publications LA-UR-03-1987, LA-CP-03-0245, and LA-CP-03-0284.